Computing the reconnection rate at the Earth's magnetopause using two spacecraft observations

S. A. Fuselier, K. J. Trattner, and S. M. Petrinec
Lockheed Martin Advanced Technology Center, Palo Alto, California, USA

C. J. Owen
Mullard Space Science Laboratory, University College London, Surrey, UK

H. Rème
CESR/CNES, Toulouse, France

Received 24 September 2004; revised 25 February 2005; accepted 13 March 2005; published 24 June 2005.

[1] A new multispacecraft technique is introduced which, under some restrictive assumptions and conditions, provides a snapshot of the reconnection inflow velocity into the magnetosphere and an estimate of the distance from the spacecraft to the reconnection site. The two quantities are not obtained independent of one another and additional, independent information is needed to separate them. This new technique is applied to Cluster spacecraft observations at the Earth's magnetopause. Additional Cluster observations and observations from the IMAGE spacecraft are used as independent information to provide an estimate of the distance from the spacecraft to the reconnection site for the event. From this distance estimate and the new multispacecraft technique, it is concluded that component reconnection was probably occurring at the magnetopause and that the local inflow velocity was significantly less than 0.1 V_A.

Citation: Fuselier, S. A., K. J. Trattner, S. M. Petrinec, C. J. Owen, and H. Rème (2005), Computing the reconnection rate at the Earth's magnetopause using two spacecraft observations, *J. Geophys. Res.*, *110*, A06212, doi:10.1029/2004JA010805.

1. Introduction

[2] Magnetic reconnection is an important process for transferring solar wind plasma into the Earth's magnetosphere. Evidence for this process is found at the Earth's magnetopause and in the magnetospheric cusps. At the magnetopause, the evidence typically consists of one or more of the following: a nonzero normal component to the magnetic field [e.g., *Sonnerup et al.*, 1981], flow velocities of ions (or electrons) that satisfy certain jump conditions across the boundary [e.g., *Sonnerup et al.*, 1981; *Paschmann et al.*, 1986], and ion and electron distribution functions that are consistent with transmission and reflection of solar wind and magnetospheric ion and electron populations across an "open" magnetopause boundary [e.g., *Sonnerup et al.*, 1981; *Fuselier et al.*, 1991, 1995]. In the Earth's magnetospheric cusps, the evidence consists of dispersive ion and electron signatures consistent with entry and acceleration of magnetosheath plasma across an open magnetopause [e.g., *Lockwood and Smith*, 1996].

[3] Although there is a wide variety of evidence for magnetic reconnection at the Earth's magnetopause, key quantitative information about the process remains poorly known. Two poorly known quantities are the location of the reconnection site (or sites) at the magnetopause and the local transfer rate of plasma across the magnetopause at the reconnection site. These quantities remain poorly known because the reconnection diffusion region is small compared with the total area of the magnetopause and spacecraft typically cross the magnetopause some (unknown) distance from the diffusion region.

[4] Without direct knowledge of the location of reconnection at the magnetopause, two basic models have been developed. These two models can differ significantly when the interplanetary magnetic field (IMF) has a southward ($-B_z$) component. In the first model, reconnection occurs at or very near those regions where the magnetic field lines in the magnetosheath are antiparallel to the magnetic field lines in the magnetosphere [e.g., *Crooker*, 1979]. In the second model, reconnection occurs along a line that is hinged in the subsolar region and has a north-south tilt that depends on the relative magnitudes of the IMF B_y and B_z components [*Sonnerup*, 1974; *Gonzalez and Mozer*, 1974]. There is observational evidence for both antiparallel and tilted neutral line (or, more generally, component) reconnection [e.g., *Sonnerup et al.*, 1981; *Gosling et al.*, 1990; *Onsager and Fuselier*, 1994]. Because in situ observations at the magnetopause are not made at the reconnection site (where the external and internal magnetic field orientations would be known directly from the observations), this evidence remains indirect and it is not known if either of these types of reconnection dominates at the magnetopause.

[5] Quantifying the rate of transfer of plasma across the boundary (the reconnection rate) has also proved to be very difficult. The relative transfer rate is related to the dimen-

0148-0227/05/2004JA010805$09.00

sionless quantity V_n/V_A, where V_n is the inflow velocity normal to the magnetopause boundary and V_A is the Alfvén speed in the magnetosheath ($=B_o/\sqrt{\mu_o\rho}$, where B_o is the magnetosheath magnetic field and ρ is the mass density). Limited case studies suggest that this ratio should be <0.1 [*Sonnerup and Ledley*, 1979]. For a typical Alfvén speed of ~250 km/s at the magnetopause and $V_n/V_A < 0.1$, the inflow velocity, V_n, is <25 km/s.

[6] At the magnetopause, the quantity B_n/B_o, where B_n is the normal component of the magnetic field at the boundary and B_o is the total magnetic field, is proportional to V_n/V_A. However, measuring a normal component that is of the order of 10% of the total field requires knowledge of the boundary normal to an accuracy of better than a few degrees. Fluctuations in the observed field strength and direction across the boundary typically result in magnetopause normals with uncertainties larger than a few degrees. Multispacecraft observations have improved the determination of the magnetopause normal [e.g., *Dunlop et al.*, 2001]. Although difficult to measure, a nonzero B_n has been measured for some magnetopause crossings [e.g., *Sonnerup et al.*, 1981; *Phan et al.*, 2001]. For these few cases, B_n/B_o (and therefore V_n/V_A) was ~0.1–0.2. These results do not represent a statistical survey of reconnection inflow at the magnetopause and may be biased to instances when the normal component of the magnetic field was large enough to be measured.

[7] Direct measure of the inflow velocity, V_n, is even more difficult than measuring the normal magnetic field. First, measuring V_n requires knowledge of the magnetopause normal to within a few degrees. The normals are usually obtained from magnetic field measurements, so this method for determining the inflow rate has the same difficulties associated with the measurement of B_n/B_o. Furthermore, the magnetopause is most often in motion with velocities comparable to the expected maximum inflow velocity of ~25 km/s [*Phan and Paschmann*, 1996]. A spacecraft measures the total velocity in the spacecraft frame of reference, which is a combination of the inflow velocity and the velocity of the magnetopause. Thus determining the inflow velocity also requires accurate determination of the magnetopause velocity. Because of these restrictions, direct measure of the inflow velocity has been attempted in only a few cases where the magnetic field normal component was also large [e.g., *Sonnerup et al.*, 1981; *Phan et al.*, 2001]. In contrast to these few cases with $V_n/V_A \sim 0.1$, a statistical study of magnetopause motion demonstrated that the magnetopause velocity usually dominates the normal velocity in the spacecraft frame and therefore V_n/V_A may be substantially smaller than 0.1 [*Phan and Paschmann*, 1996].

[8] Another way to estimate the inflow velocity at the magnetopause is to determine the tangential electric field, E_t. Similar to the determination of V_n, the determination of E_t requires transformation into the frame of reference where the normal velocity of the magnetopause is zero. Thus accurate determination of E_t suffers from the same uncertainties as the direct determination of V_n. A survey of the electric field measurements at the magnetopause near the subsolar region yielded an estimate of $V_n/V_A \sim 0.15$ [*Lindqvist and Mozer*, 1990]. However, there was significant scatter in these measurements and E_t was derived assuming that the magnetopause normal and velocity were constant. It is not clear if the scatter was due to true variations in V_n or due to the simplifying assumptions used to derive E_t. Finally, detailed analysis of the electric field observed during a single crossing of the magnetopause very near the diffusion region yielded an inflow rate of ~0.02 V_A [*Mozer et al.*, 2002].

[9] To summarize, indirect measure of the inflow velocity suggests that it can be ~0.1–0.2 V_A, in agreement with the upper limit provided by theory [e.g., *Levy et al.*, 1964]. Direct measure of the inflow velocity for a few cases yields a similar value. However, study of the magnetopause motion and other indirect measure of the inflow velocity also suggest that this velocity could be substantially smaller than 0.1 V_A.

[10] This paper introduces a new, multispacecraft technique for determining the location of the reconnection site and the inflow velocity at the magnetopause. After introducing the technique in section 2, it is applied to ion observations from the Cluster spacecraft in section 3. The location of the reconnection site and the inflow velocity are not determined independent of one another. Therefore additional information is needed to separate them. Additional information from the Cluster spacecraft and from the IMAGE spacecraft is used in section 4 to estimate the distance to the reconnection site for the example event. Section 5 discusses the inflow velocity and section 6 discusses the conclusions. From the independent distance determination, it is concluded that component (tilted neutral line) reconnection was probably occurring at the magnetopause. Furthermore, the inflow speed for this component reconnection event was significantly less than 0.1 V_A.

2. Multispacecraft Technique

[11] The multispacecraft technique introduced here requires observations from at least two spacecraft that are in a reconnection layer at the same time. Although the derivation is valid on either side of the magnetopause, the focus here is on the reconnected field lines on the earthward side of the magnetopause in the low-latitude boundary layer. In this layer it is assumed that reconnection occurs at the same rate along a long neutral line at the magnetopause. The neutral line is assumed to be at least as long as the spacecraft separation parallel to the line. With these assumptions, the reconnection geometry and the spacecraft locations in the reconnection layer can be reduced to a two-dimensional geometry (see Figure 1). In Figure 1, spacecraft 1 (2) is located a distance X_1 (X_2) from the magnetopause and a distance Y_1 (Y_2) from the reconnection line. The spacecraft may be separated in the Z direction (the direction out of the plane of Figure 1), but the above assumptions about the reconnection rate and neutral line reduce the geometry to two dimensions.

[12] Figure 1 is a snapshot of the two-dimensional magnetic field configuration. The magnetic field lines reconnect at the bottom of the figure. Plasma on these field lines receives significant energization (proportional to the Alfvén speed). The newly reconnected field lines propagate along the magnetopause at the deHoffman-Teller velocity (V_{dHT}) and it is assumed here that this velocity is also constant along the magnetopause. The ion velocity in the layer can

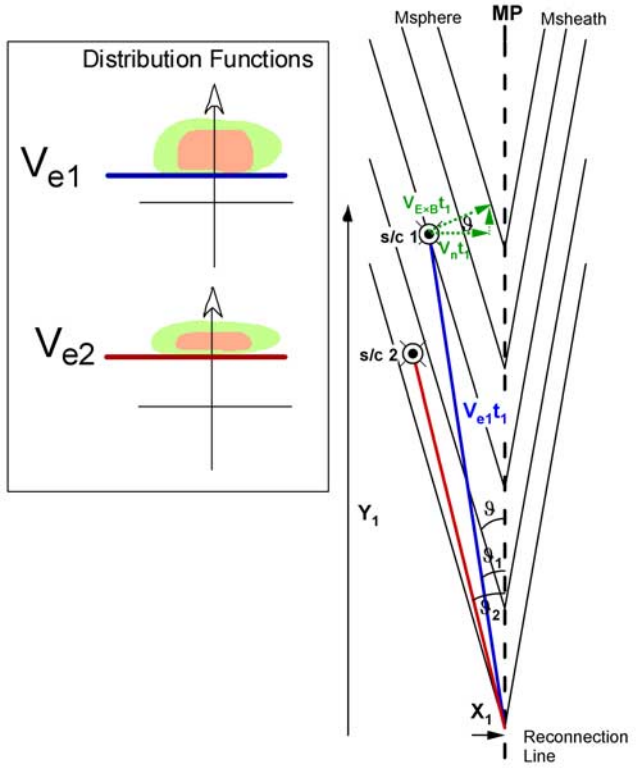

Figure 1. Two-dimensional geometry used to compute the inflow velocity and the distance to the reconnection line given two spacecraft observations in the reconnection layer. For the spacecraft locations in the layer, the velocity distributions in the spacecraft reference frame will resemble those in the inset. In particular, the cutoff velocity (V_{e1}) for spacecraft 1 will be lower than that for spacecraft 2 because spacecraft 2 is closer to the edge of the reconnection layer (defined as the magnetic field line directly connected to the reconnection line). The blue and red lines emanating from the reconnection site show the trajectories of these ions moving at the cutoff velocity.

be decomposed into flow along and across the magnetic field. Ions move along the magnetic field in the Y direction at a fairly high speed (because of their energization in the reconnection process). They also move along the magnetic field in the $-X$ direction (away from the magnetopause) with a relatively low velocity (because the field makes a small angle ϑ with the magnetopause). These ions experience an $\mathbf{E} \times \mathbf{B}$ drift across the field which caries the ions along the magnetopause (in the Y direction) and back toward the magnetopause (in the X direction) at a very low velocity. The inflow velocity in the X direction, V_n, is assumed to be constant all along the magnetopause.

[13] To enter the boundary layer, ions must have a velocity in the $-X$ direction that exceeds V_n. Typically, the velocity in the Y direction is of the order of the Alfvén speed or ~200–300 km/s. The magnitude of V_n was discussed in the introduction and is ~0.1–0.2 V_A or 20–60 km/s. The speed into the boundary layer in the $-X$ direction can be any value as long as it exceeds V_n.

[14] Because shocked solar wind plasma crosses all along the magnetopause and the magnetic field and plasma convect in the direction normal to the boundary, there are time-of-flight effects in the ion distributions. Below a certain cutoff velocity, ions cannot arrive at the spacecraft location and are not observed. The magnitude of this cutoff velocity is related to the distance from the spacecraft to the magnetopause and from the spacecraft to the reconnection line. If a spacecraft is very close to the magnetopause and relatively far from the reconnection line, then this cutoff velocity is low (for small angle ϑ, the cutoff velocity near the magnetopause is the deHoffman-Teller velocity, V_{dHT}) [e.g., *Cowley*, 1982]. If a spacecraft is located at the edge of the reconnection layer (on the field line directly connected to the reconnection line at the bottom of Figure 1), then the cutoff velocity is infinite. In Figure 1, the blue and red lines in the inset distributions show the cutoff velocities for spacecraft 1 and 2, respectively. In the snapshot of the reconnection layer, similar blue and red lines show the trajectories of ions moving at the cutoff velocities to arrive at spacecraft 1 and 2.

[15] At spacecraft "i", the X and Y velocities of an ion moving at the cutoff velocity (V_{ei}, where the subscript "e" is borrowed from *Fuselier et al.* [2000] and refers to the earthward propagating ion population in the LLBL) are

$$V_{yi} = V_{ei}\cos\vartheta + V_{\mathbf{E}\times\mathbf{B}}\sin\vartheta \tag{1}$$

$$V_{xi} = V_{ei}\sin\vartheta - V_{\mathbf{E}\times\mathbf{B}}\cos\vartheta. \tag{2}$$

[16] Using the relationship $V_n = V_{\mathbf{E}\times\mathbf{B}}\cos\vartheta$ (Figure 1), these two equations are rewritten as

$$V_{yi} = V_{ei}\cos\vartheta + V_n\sin\vartheta/\cos\vartheta \tag{3}$$

$$V_{xi} = V_{ei}\sin\vartheta - V_n. \tag{4}$$

The ratio of the X and Y velocities is equal to the ratio of the distances X and Y from the magnetopause and the reconnection site, respectively. This ratio is

$$\frac{X_i}{Y_i} = \frac{V_{xi}}{V_{yi}} = \frac{V_{ei}\sin\vartheta - V_n}{V_{ei}\cos\vartheta + V_n\sin\vartheta/\cos\vartheta}. \tag{5}$$

[17] A key assumption to simplify equation (5) is that the angle ϑ is small. For small ϑ, then $\cos\vartheta \sim 1$ and $V_n\sin\vartheta \ll V_{ei}$. In this limit, equation (5) becomes

$$\frac{X_i}{Y_i} = \frac{V_{xi}}{V_{yi}} \cong \sin\vartheta - \frac{V_n}{V_{ei}}. \tag{6}$$

However, from the tangential stress balance condition [e.g., *Sonnerup et al.*, 1981], $\sin\vartheta = V_n/V_A$, (and $\approx B_n/B_o$), where V_A is the Alfvén speed. Here, it is apparent that the small angle assumption simply implies that V_n/V_A is small (i.e., V_n/V_{A} < approximately 0.2). Thus equation (6) becomes

$$\frac{X_i}{Y_i} = \frac{V_{xi}}{V_{yi}} \cong \frac{V_n}{V_A} - \frac{V_n}{V_{ei}}. \tag{7}$$

[18] Equation (7) has a simple interpretation. The cutoff velocity must be greater than the local Alfvén speed for the

ion population to be seen some distance from the magnetopause in the boundary layer. In the limit that the cutoff velocity becomes infinite, the ions move along the first reconnected field line in Figure 1 away from the reconnection layer.

[19] Using the definitions of the positions of the spacecraft relative to one another,

$$X = X_2 - X_1 \tag{8}$$

$$Y = Y_2 - Y_1. \tag{9}$$

Equation (7) for spacecraft 1 and 2 can be solved separately for the X_1 and Y_1 (i.e., the location of spacecraft 1 relative to the magnetopause and the reconnection line). The location of the spacecraft relative to the reconnection line is written in terms of the relative separations of the spacecraft (X and Y), the cutoff velocities measured at the two spacecraft (V_{e1} and V_{e2}), the local Alfvén speed, V_A, and the inflow velocity V_n:

$$Y_1 = \frac{V_{e1}V_{e2}}{V_{e1} - V_{e2}}\left(\frac{X}{V_n} - Y\left(\frac{1}{V_A} - \frac{1}{V_{e2}}\right)\right) \tag{10}$$

$$X_1 = Y_1 V_n\left(\frac{1}{V_A} - \frac{1}{V_{e1}}\right). \tag{11}$$

[20] By measuring the cutoff velocity in the frame of reference where the perpendicular flow velocity is nearly zero, the magnetopause motion is effectively removed from the equations of motion of the ions in the spacecraft rest frame. Thus unlike the direct measure of V_n or the tangential electric field, E_t, discussed in the introduction, this technique for determining the inflow velocity does not require direct measure of the normal component of the magnetopause velocity.

[21] Although the multispacecraft method described here has the advantage of removing the need to determine the magnetopause velocity, it suffers from four shortcomings that limit its use. First, it is still necessary to determine the normal to the magnetopause. Thus this technique has the same issues associated with determining the reconnection rate by determining B_n. The velocity cutoffs used in equations (4) and (5) may be less sensitive to the direction of the normal component than the direct determination of B_n. Furthermore, there is an independent way to test the validity of the normal component. The direction of the normal component determines the relative spacecraft separation in the X and Y directions. However, the cutoff velocities also indicate the relative positions of the spacecraft within the layer (the higher cutoff velocity is observed on the spacecraft closer to the inner edge of the reconnection layer). Therefore the normal direction determined from the magnetic field must be consistent with the different times-of-flight of the ions from the reconnection line. The sensitivity of this method to the determination of the normal direction has not been investigated and is beyond the scope of this paper.

[22] The second shortcoming is that the spacecraft must be sufficiently far apart so that the cutoff velocities V_{e1} and V_{e2} differ by a significant amount. These cutoff velocities are subtracted from one another in the denominator of equation (10), so their difference must be significantly larger than the uncertainties in their measurement. The problem is analogous to the distance determination using cutoff velocities of the incident and reflected populations in the cusp [e.g., *Fuselier et al.*, 2000; *Trattner et al.*, 2004]. For the cusp measurements and for the measurements in equation (10), the difference in the cutoff velocities should be of the order of several hundred km/s because uncertainties in the cutoff velocities are typically of the order of 50 km/s. For narrow reconnection layers at the magnetopause produced by low reconnection rates, it may not be possible to find intervals when the spacecraft are sufficiently separated and the spacecraft are still in the boundary layer.

[23] The third shortcoming is the limiting assumptions used to derive equation (10). Particularly important are the assumptions that the reconnection rate and the Alfvén speed are constant along the magnetopause from the reconnection site to the spacecraft. These assumptions may be true for reconnection sites relatively close to the spacecraft. However, the two spacecraft technique is better suited for reconnection sites relatively far from the spacecraft because the boundary layer thickness increases with distance from the reconnection site. The small angle approximation used to simplify equation (5) is not very restrictive because maximum reconnection rates at the magnetopause that result in $V_n/V_A <$ approximately 0.2 will satisfy this small angle approximation. The assumption that the Alfvén speed is constant will be tested in section 5 and it will be shown that this assumption is also not very restrictive.

[24] Finally, the fourth shortcoming is that in equation (10), the location of the spacecraft in the reconnection layer depends on another unknown quantity, V_n, the inflow velocity. This result has the simple interpretation that with two spacecraft, it is not possible to determine if the spacecraft are relatively close to the reconnection line and the inflow velocity is high or if the spacecraft are relatively far from the reconnection line and the inflow velocity is low. Additional information is required to distinguish these two possibilities and determine separately the distance to the reconnection site and the inflow velocity. This additional information may not always be available.

[25] In the next section, equation (10) is applied to an example event. The additional information needed to determine separately the distance to the reconnection line and the inflow velocity is introduced in section 4.

3. Cluster Observations in the LLBL on 11 January 2002

[26] The Cluster mission provides an excellent opportunity to test the multispacecraft technique introduced in the previous section. To conduct this test, an event is needed where two (or more) spacecraft are in the reconnection layer and are separated by a large enough distance such that the cutoff velocities measured at the two spacecraft are sufficiently different.

[27] During the months of January and February 2002, the Cluster configuration and spacecraft separations were adjusted. Over this time period, the spacecraft were often not in the nominal tetrahedron configuration and there were

Table 1. Important Quantities for the Boundary Layer/Magnetosheath Interval at 0651 UT

Quantity	Value
GSM location of the magnetopause crossing, R_E	2.91, 8.67, 8.66
GSM Magnetopause model normal	0.579, 0.577, 0.576
Spacecraft 4–1 separation (X,Y coordinates from Figure 1), R_E and km	−0.02, −0.317 R_E 126, −2021 km
GSM Average magnetic field orientation in the magnetosheath, nT	4, 15, −15
Alfvén speed, V_A, km/s	140

often relatively large separations between some of the spacecraft. Approximately 14 intervals containing multiple encounters with the magnetopause were surveyed during this interval to find an event where two spacecraft were sufficiently separated in the boundary layer during a reconnection event. An event on 11 January 2002 fits these criteria.

[28] On 11 January 2002, the spacecraft crossed the magnetopause a number of times from 0645 to 0715 UT. The crossings occurred at high northern latitudes on the duskside magnetopause. Table 1 lists relevant parameters for the crossing that occurred at about 0650 UT.

[29] Because of the relatively large spacecraft separations, there were frequent instances when one or more spacecraft were in the magnetosheath while other spacecraft were in the low-latitude boundary layer (LLBL) or magnetosphere. The magnetic field changes for many of the crossings into the LLBL or magnetosheath resemble so-called "crater" flux transfer events (FTEs) [*Farrugia et al.*, 1988]. Using electron and ion measurements from the Cluster spacecraft, it was shown that the differences in the FTE structures seen at individual spacecraft were simply a function of the depth of penetration of the spacecraft into the boundary layer (C. Owen, personal communication, 2004).

[30] Here data from the Cluster Ion Spectrometer (CIS) Composition and Distribution Function (CODIF) experiments [*Rème et al.*, 2001] on spacecraft 1, 3, and 4 are used from one of these boundary layer/magnetopause crossings. Figure 2 shows an overview of the crossing. The three parts show the energy time flux spectrograms of protons from ~20 eV/e to ~35 keV/e. All three spacecraft start and end in the magnetosphere. Over the 10 min interval, the spacecraft penetrate at different depths into the boundary layer/magnetopause. Spacecraft 4 briefly encounters the LLBL at 0652 UT. Spacecraft 1 penetrates deeper into the boundary layer over the period from 0651 UT to 0652:30 UT and remains in the magnetosphere thereafter. Spacecraft 3 goes completely through the LLBL, across the magnetopause, and spends most of the time between about 0650:30 UT and 0655 UT in the magnetosheath. This spacecraft returns to the magnetosphere and makes another magnetopause crossing before returning to the magnetosphere at the end of the interval.

[31] The depth of penetration into the boundary regions is related to the relative locations of the spacecraft. For the model magnetopause normal in Table 1, spacecraft 3 is furthest from the Earth, followed by spacecraft 1 and then

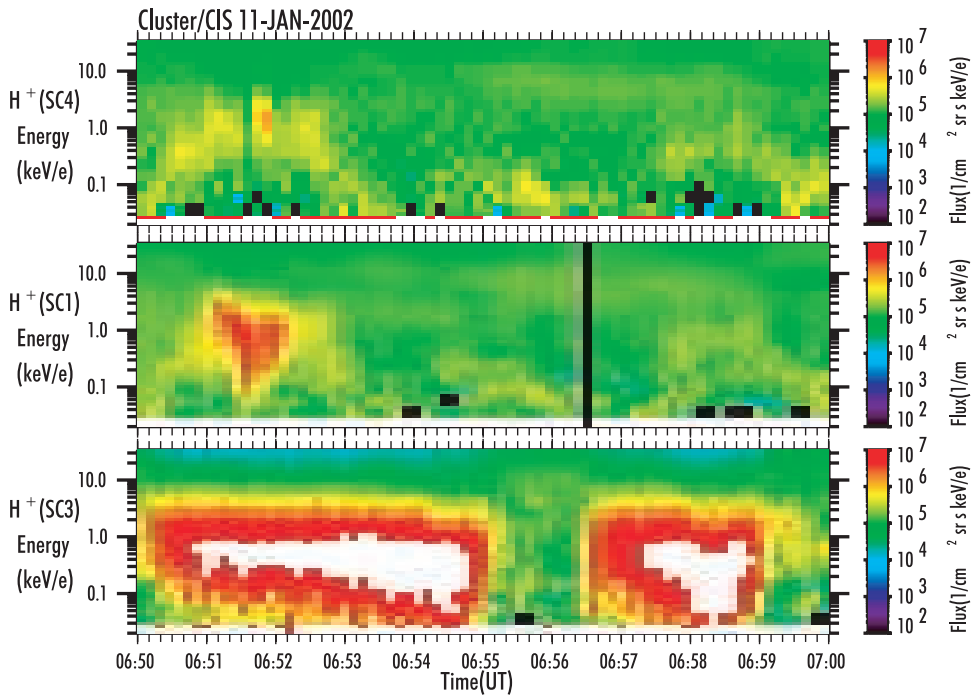

Figure 2. Cluster Ion Spectrometer (CIS) observations of boundary layer/magnetopause crossings on 11 January 2004. The three spacecraft start and end in the magnetosphere. Spacecraft 3, furthest from the Earth, enters the low level boundary layer (LLBL) at 0650 UT, crosses the LLBL and remains in the magnetosheath until 0655 UT. This spacecraft is back in the LLBL/magnetosheath from 0656:30 UT to 0659 UT. Spacecraft 1, closer to the Earth, crosses into the boundary layer from 0651 to 0652:30 UT. Finally, spacecraft 4, closest to the Earth, makes only a brief crossing into the boundary layer at about 0652 UT.

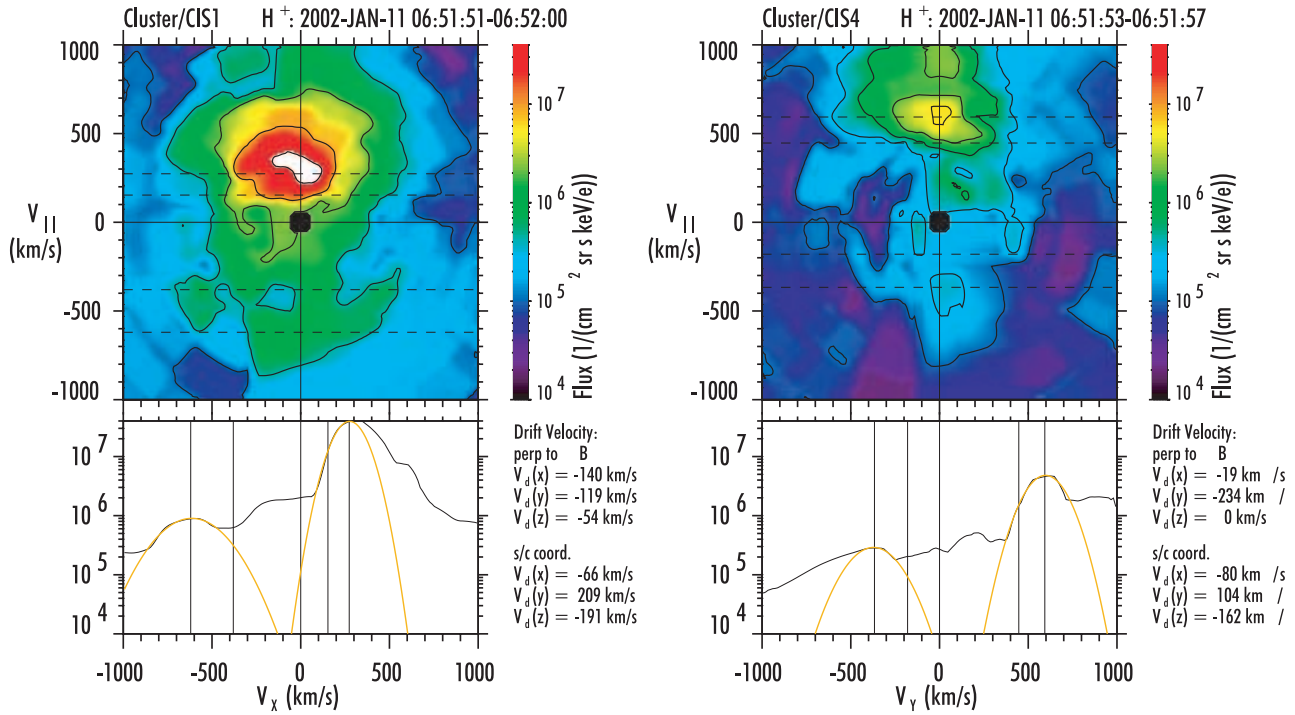

Figure 3. Cluster 1 (left) and 4 (right) spacecraft observations in the boundary layer. The top parts show the velocity space distributions in the frame where the bulk flow perpendicular to the magnetic field is zero. The bottom parts show cuts parallel to the magnetic field. Both distributions show velocity cutoffs parallel to the magnetic field. The cutoff velocity for spacecraft 4 (near the inner edge of the boundary layer) is higher than that of spacecraft 1 (near the magnetopause).

spacecraft 4. Spacecraft 1 and 4 are separated by only 126 km (Table 1) in the magnetopause normal direction. Nonetheless, their relative penetration into the LLBL is quite different (Figure 2). This difference will be attributed to their relative separation parallel to the magnetopause.

[32] Figure 3 shows velocity space distributions from spacecraft 1 and 4 from the LLBL interval between 0650 and 0652 UT. The top parts show contours of constant flux with two contours per decade. These distributions were obtained by first transforming into the frame of reference where the velocity perpendicular to the local magnetic field is zero. This frame is determined from the velocity space moments of the ion distribution and the local magnetic field direction measured by the Cluster spacecraft magnetometers [*Balogh et al.*, 1997]. In this frame, the distributions in Figure 3 are obtained by first selecting a plane containing the velocity parallel to the magnetic field. Then, by preserving the proton pitch angle, all measurements within ±45° of the selected plane are rotated into that plane. The orientation of the plane is arbitrary and the cutoff velocity discussed below is independent of this orientation. The bottom parts show cuts through these distributions along the magnetic field direction.

[33] The distributions in Figure 3 resemble those illustrated in the inset in Figure 1. In particular, they both have an ion population propagating parallel to the magnetic field at relatively high velocity. These ion populations have a cutoff velocity parallel to the magnetic field. In Figure 3, the observed cutoff velocity for spacecraft 4 is significantly higher than that for spacecraft 1 (this result is also evident in the energy-time spectrograms for spacecraft 1 and 4 in Figure 2). Thus from these distributions in Figure 3 and the cartoon in Figure 1, it is concluded that the two spacecraft are located in a reconnection layer where the reconnection site is below (equatorward) of the spacecraft location. Furthermore, spacecraft 4 is located somewhat closer to the inner edge of the reconnection layer than spacecraft 1 (i.e., in Figure 1 the spacecraft labeled 2 is Cluster spacecraft 4 and the spacecraft labeled 1 is Cluster spacecraft 1). The relative separations of the spacecraft are shown in Table 1.

[34] In Figure 3, the cutoff velocities estimated from the ion distributions observed by spacecraft 4 and 1 are 450 ± 50 km/s and 150 ± 50 km/s, respectively. These cutoff velocities are determined by fitting a Maxwellian to the parallel propagating ion distribution and choosing the cutoff to be the velocity where the flux reaches 1/e of peak. This same technique has been applied to cusp ion distributions to determine their cutoff velocities [e.g., *Trattner et al.*, 2004]. Using these cutoff velocities from Figure 3, the relative separations of the spacecraft from Table 1, and equation (10), Figure 4 shows the distance from the reconnection site to spacecraft 1 as a function of the inflow velocity, V_n. Error bars are derived from the uncertainties in the cutoff velocities.

[35] Figure 2 shows that spacecraft 4 remained in the boundary layer only a short time. The CIS instrument measured two ion distributions during this brief period. A similar calculation using equation (4) was done using the second ion distribution measured by spacecraft 4 and its corresponding distribution measured by spacecraft 1. The

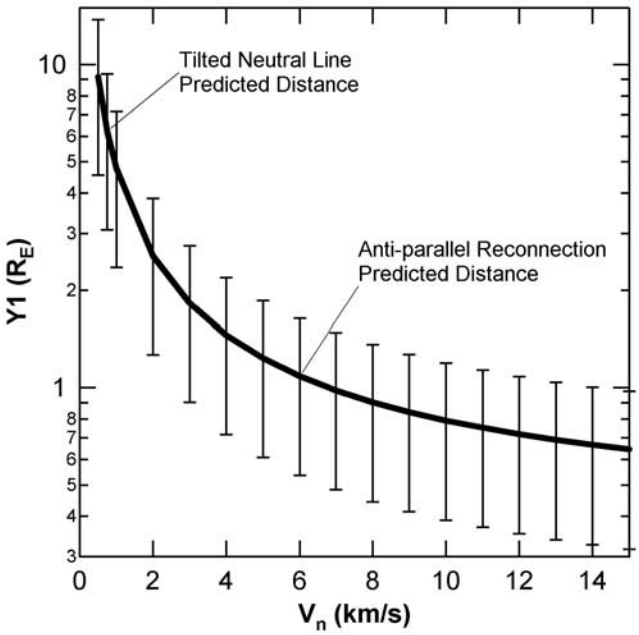

Figure 4. Spacecraft 1 distance from the reconnection site as a function of the normal (inflow) velocity at the magnetopause for the LLBL event in Figure 2. The distances to the reconnection site for tilted neutral line (component) reconnection and antiparallel reconnection were obtained by modeling the magnetosheath and magnetospheric magnetic field conditions for the event. For tilted neutral line reconnection, the reconnection site is quite far from the spacecraft and the inflow speed is very low.

results (not shown) are similar to those shown in Figure 4. Specifically, the inflow velocity was between 1 and 20 km/s and spacecraft 1 was between 10 and <1 R_E from the reconnection site.

[36] As discussed in context with the derivation of equation (4), it is not possible to determine if the spacecraft are relatively near the reconnection line ($Y_1 < 1\ R_E$) and the inflow velocity is large ($V_n \sim 10-20$ km/s) or if they are relatively far from the reconnection line ($Y_1 \sim 10\ R_E$) and the inflow velocity is small ($V_n \sim 0.5-1$ km/s). Additional information used to distinguish these two possibilities is discussed in the next section.

4. Independent Estimate of the Distance to the Reconnection Site

[37] In this section, two pieces of additional information are used to determine the distance to the reconnection site. One piece of information comes from the Cluster spacecraft and one comes from the IMAGE spacecraft. The precise distance is not determined from these data. Rather, they are used to distinguish between two competing models for reconnection at the magnetopause, the tilted neutral line and the antiparallel models.

[38] The first piece of information available from the Cluster spacecraft results in a very qualitative measure of the distance to the reconnection site. Figure 5 shows the flow velocities of spacecraft 1 and 3 for the 10 min time interval in Figure 2. During the period from 0651 UT to 0652:30 UT, spacecraft 3 was in the magnetosheath and spacecraft 1 was in the LLBL. Spacecraft 3 observes a $-V_x$, $+V_y$, $+V_z$ flow. This tailward/duskward/poleward flow is consistent with the spacecraft location in the magnetosheath near the northern high-latitude duskside magnetopause. In contrast, spacecraft 1 in the LLBL observes a $-V_y$ flow, opposite that of spacecraft 3. (The LLBL flow is also accelerated in the $+V_z$ direction relative to the magnetosheath due to the reconnection.) The top parts of Figure 6 show how the change in the V_y flow across the magnetopause is consistent with the tilted neutral line model and inconsistent with the antiparallel model.

[39] The top parts of Figure 6 show the predicted locations of the reconnection neutral lines for the antiparallel model (left) and the tilted neutral line model (right). These predicted locations were obtained by determining the global pattern of model magnetosheath and magnetospheric field lines. The model magnetospheric field lines were obtained from the Tsyganenko 96 [*Tsyganenko*, 1995] model. The model magnetosheath field lines were obtained by propagating the solar wind magnetic field orientation from the ACE spacecraft to the bow shock using the solar wind velocity measured at ACE, then deriving the magnetosheath field orientation (and magnitude), using the *Kobel and Flückiger* [1994] model. The propagation time from ACE to the bow shock was then adjusted (by a few minutes) until the model magnetic field orientation matched the orientation observed at the Cluster 3 spacecraft location (in the magnetosheath at 0652 UT). For antiparallel reconnection at the magnetopause, the locations of the reconnection lines (up-

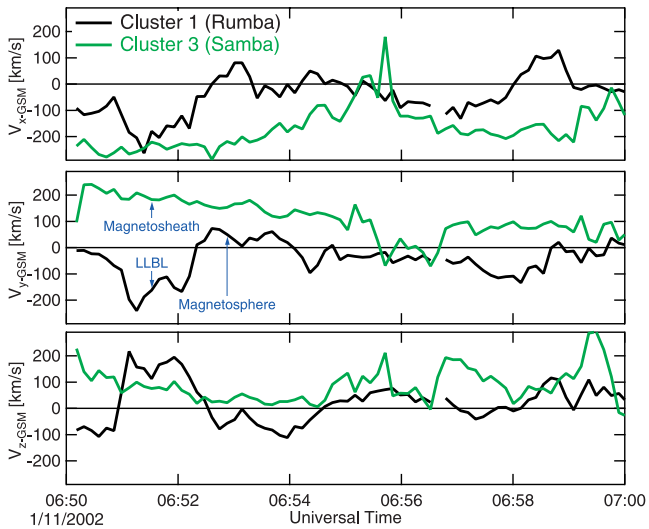

Figure 5. Cluster spacecraft 1 (black lines) and 3 (green lines) bulk flow velocity components in GSM coordinates. During the brief interval from 0651 to 0652:30 UT, spacecraft 3 was in the magnetosheath and spacecraft 1 was in the LLBL. The flow in the LLBL is accelerated relative to the flow in the magnetosheath, especially in the V_z direction. Furthermore, the flow in the LLBL is reversed in the V_y direction. In the magnetosheath, the flow is consistent with the shocked solar wind flow around the magnetospheric obstacle. In the LLBL, the reversal of the flow is consistent with reconnection at a tilted neutral line hinged at the subsolar point.

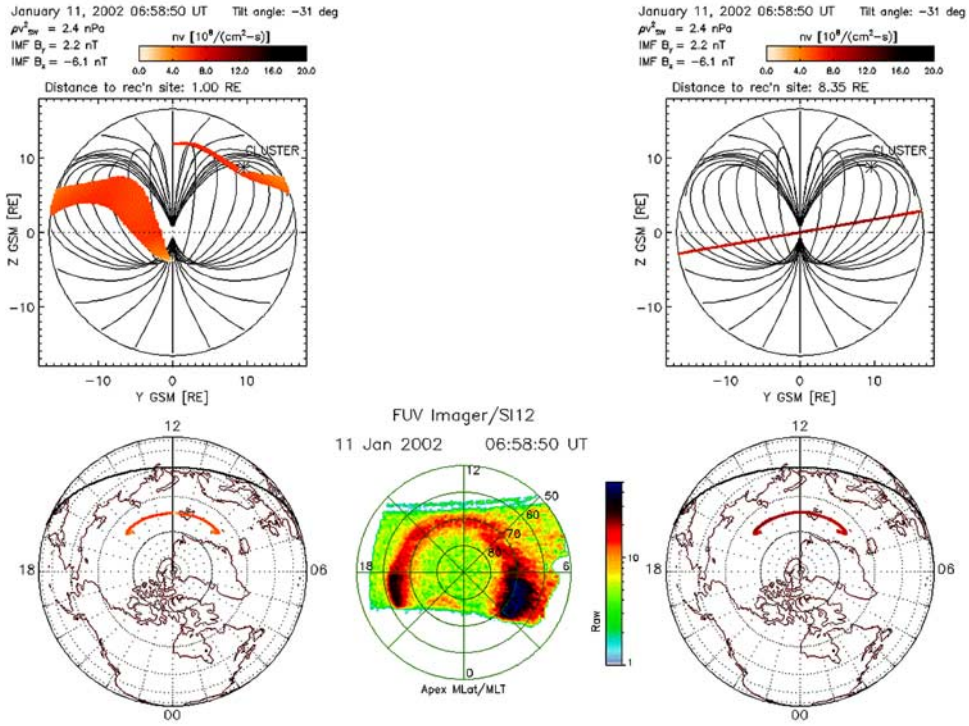

Figure 6. Predictions and observations of the ionospheric footpoint of reconnected flux tubes for the event in the paper. The top parts show the location of anti-parallel (left-hand side) and tilted neutral line (right-hand side) reconnection sites on the magnetopause. The view is from the Sun along the Earth-Sun line. The intensity of the reconnection line is proportional to the proton flux into the ionosphere. Model magnetic field lines inside the magnetosphere and the position of the Cluster 3 spacecraft in the magnetosheath are shown. The bottom parts show (left to right), the predicted footpoint of the anti-parallel reconnection sites in the ionosphere, the observed proton aurora from the IMAGE spacecraft, and the predicted footpoint of the tilted neutral lines reconnection site in the ionosphere. These predictions and observations are shown in magnetic local time-invariant latitude coordinates. The intensity is proportional to the flux of protons into the ionosphere. The predicted footpoint for antiparallel reconnection shows a gap in the precipitation from about 1130 to 1200 MLT. The observed ionospheric precipitation is more consistent with the tilted neutral line prediction, which does not show a gap near noon.

per left part of Figure 6) were determined by finding places on the magnetopause where the draped magnetosheath field was antiparallel to the magnetospheric field. Because of the $+B_y$ component in the solar wind, the reconnection site is split at noon. The basic orientation of the antiparallel reconnection sites is consistent with that of *Crooker* [1979]. Modifications to these early predictions include the addition of a relatively large dipole tilt on 11 January 2002 and draping of a model magnetic field against a realistic magnetopause model. The high-latitude reconnection site on the duskside is predicted to be very close to the Cluster 3 spacecraft. For tilted neutral line reconnection at the magnetopause, the location of the reconnection line (upper right part of Figure 6) was determined by hinging the neutral line at the subsolar point and tilting it at the appropriate angle based on the value of B_y [e.g., *Sonnerup*, 1974].

[40] The tilted neutral line (right side) is oriented such that reconnected field lines in the northern hemisphere duskside will peel off in the $-V_y$ direction. In the LLBL inside the magnetosphere, the plasma is predicted to have a $-V_y$ flow. Such "flow reversal" events have been observed and interpreted in this fashion [*Gosling et al.*, 1990]. In contrast, the orientation of the antiparallel neutral line in the northern hemisphere on the duskside is opposite that of the tilted neutral line. For antiparallel reconnection, the reconnected field lines in the northern hemisphere on the duskside will peel off in the $+V_y$ direction. In the LLBL inside the magnetosphere, the plasma is predicted to have a $+V_y$ flow (i.e., in the same direction as the magnetosheath flow outside). Thus comparison of the flow velocities measured simultaneously in the LLBL and the magnetosheath for this event (Figure 5) with model predictions (Figure 6) suggests that tilted neutral line (component) reconnection is occurring at the magnetopause.

[41] In Figure 6, the reconnection site for the tilted neutral line is quite far (>8 R_E) from the Cluster spacecraft. This distance, as well as the predicted distance for antiparallel reconnection from the upper right-hand side of Figure 6, is shown on the curve in Figure 4. For the tilted neutral line location >8 R_E from the spacecraft, the inflow velocity is predicted to be between 0.5 and 2 km/s.

[42] Additional observations from the IMAGE spacecraft are consistent with this component reconnection interpretation. Again, only a qualitative result is obtained from these observations. The bottom parts of Figure 6 show (left to right) the predicted ionospheric precipitation signatures for antiparallel reconnection, the IMAGE/FUV/SI12 observations of proton aurora during the event, and the predicted precipitation for tilted neutral line reconnection. The ion flux entering through the reconnection sites and precipitating into the ionosphere is estimated using available analytic and semiempirical models, with parameterization by upstream solar wind observations. The model magnetic fields are described above. The magnetosheath ion density is determined from hydrodynamics [*Petrinec and Russell*, 1997], as is the magnetosheath bulk flow velocity (modified by the macroscopic $\mathbf{J} \times \mathbf{B}$ force created by the presence of the magnetosphere) [*Petrinec et al.*, 1997]. With these parameters, the local Alfvén speed (V_A) and the deHoffman-Teller velocity ($\mathbf{V_{dHT}}$) at a given point on the magnetopause is estimated. The vector sum of the deHoffman-Teller velocity and the velocity along the reconnecting magnetospheric field line ($V_A\mathbf{b_{sphere}}$) provides an estimate of the flow of reconnecting plasma ($\mathbf{V_{sphere}}$). This is a generalization of the *Cowley and Owen* [1989] model. The component of this vector quantity along the magnetospheric magnetic field $(V_A\mathbf{b_{sphere}})_{||}$ multiplied by the magnetosheath ion density at the point on the magnetopause is an estimate of the particle flux entering and moving along the reconnected magnetospheric field line toward the northern ionosphere. This flux is shown in the top parts of Figure 6 color coded by intensity. Assuming that the pitch-angle extent of the ion loss cone and any field-aligned electric fields are independent of magnetic local time and that there is little evolution with time, then the ion flux entering the magnetosphere can be mapped down to the northern ionosphere using the same color coding. The resulting estimated proton precipitation pattern in invariant latitude, magnetic local time coordinates is shown in the bottom left- and right-hand sides of Figure 6. Higher fluxes are observed when the reconnection site is in the northern hemisphere and the angle between the magnetosheath and magnetospheric magnetic fields is maximum [*Petrinec and Fuselier*, 2003; *Fuselier et al.*, 2003]. The tilted neutral line model predicts continuous precipitation from 0900 to 1500 Magnetic Local Time. In contrast, the antiparallel model predicts a region of reduced flux from about 1130 to 1200 Magnetic Local Time. This "gap" results from the dip of the antiparallel neutral line below the equator on the dawnside. Ions that precipitate in the northern hemisphere but come from south of the equator will have reduced energy because these ions must overcome the southward magnetosheath flow [see *Petrinec and Fuselier*, 2003; *Fuselier et al.*, 2003].

[43] The observations of proton precipitation for this event from the IMAGE SI12 imager [*Mende et al.*, 2000] are shown in the lower middle part of Figure 6. The continuous proton precipitation across noon magnetic local time is consistent with the tilted neutral line model and inconsistent with the antiparallel model. Both models predict a small "hook" in the precipitation pattern at about 0900 MLT. This hook is seen in the observed precipitation pattern as a break in the precipitation at about 0900 MLT. This break separates the dayside precipitation (into the cusp) from the proton precipitation that has propagated from the nightside to the dawnside. In summary, the IMAGE observations of continuous dayside proton precipitation in Figure 6 are consistent with component reconnection at the magnetopause and are therefore consistent with the interpretation of the flow velocities from Cluster spacecraft 1 and 3 in Figure 5.

[44] Although the observations in Figures 5 and 6 yield only qualitative information, they suggest that the reconnection site was relatively far away from the Cluster spacecraft at the time of the magnetopause encounter. From Figure 4, the inflow velocity could have been as low as $\sim$0.5–1 km/s and the reconnection site could have been >8 R_E from the Cluster spacecraft.

5. Inflow Velocity and the Reconnection Rate

[45] By knowing the range of possible distances to the reconnection site, the inflow velocity can be compared with the local Alfvén velocity to determine V_n/V_A, which is related to the reconnection rate. Before this ratio can be computed, the local Alfvén velocity (i.e., the Alfvén velocity at the reconnection site) must be computed. The local Alfvén velocity depends on the plasma density and the magnitude of the magnetic field. Furthermore, the local Alfvén velocity associated with the reconnection rate must be computed using only the magnitude of the magnetic field that reverses across the discontinuity [e.g., *Swisdak et al.*, 2003]. Assuming that the tilted neutral line model is correct, Figure 6 (top right-hand side) shows that the Cluster spacecraft were relatively far from the reconnection site. Thus the density, magnetic field, and magnetic field orientation must be modeled to determine the Alfvén velocity at the reconnection site. This modeling serves as a check on the assumption that V_A is constant along the magnetopause from the reconnection site to the spacecraft.

[46] The density, magnetic field, and magnetic field orientation are estimated from the magnetosheath observations at the Cluster 3 spacecraft, and the magnetic field and magnetosheath plasma models described in the previous section. Figure 7 shows the results. The top part shows the variation of the number density along the magnetic field line that connects the Cluster 3 spacecraft with the tilted neutral line in Figure 6 (top right-hand side). The observed density at the Cluster 3 location (9 cm^{-3}) was used to obtain an absolute density variation from the magnetosheath plasma model. Similarly, the observed magnetic field magnitude (20 nT) was used to obtain an absolute magnetic field magnitude variation from the *Kobel and Flückiger* [1994] magnetic field model. Finally, the component of the magnetic field that reverses across the magnetopause as a function of distance from the reconnection site was determined from the angle between the model magnetosheath and magnetospheric magnetic fields. At the Cluster 3 location, the fields are nearly antiparallel, so the observed magnetic field magnitude was used. At the predicted distance of the tilted neutral line, the angle between the model magnetosheath and magnetospheric fields was $\sim$135°, so the field strength used to determine V_A there, although it should be larger because it is closer to the subsolar point than the Cluster 3 position, is reduced in Figure 7 by the cos(135°).

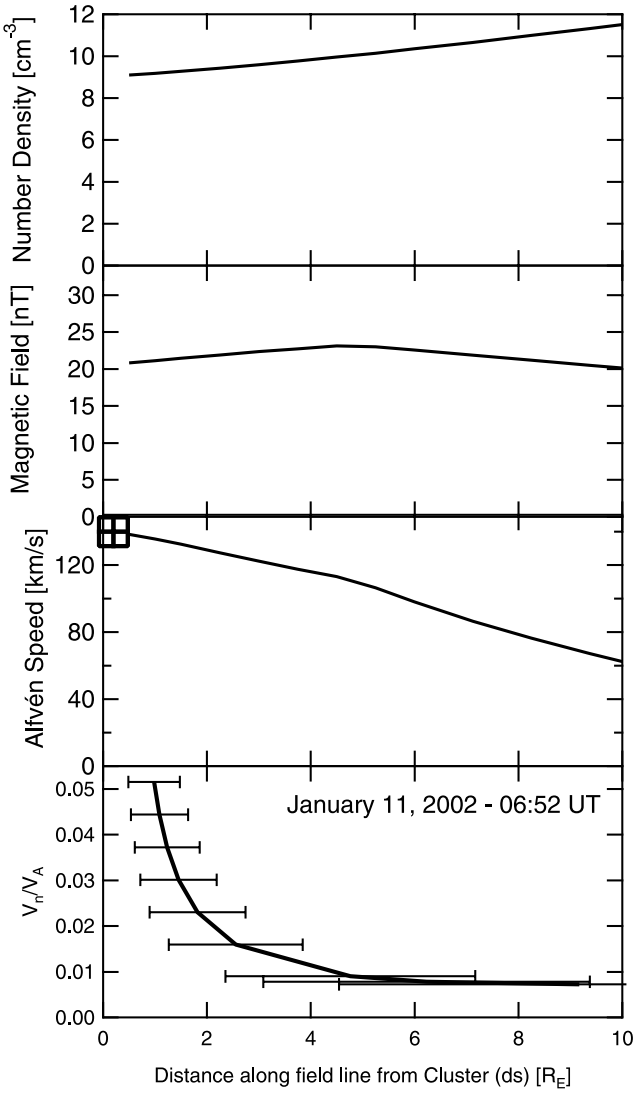

Figure 7. The number density, magnetic field strength, Alfvén speed, and V_n/V_A the (V_n from Figure 4) along the magnetospheric magnetic field line linking the Cluster 3 spacecraft location in the top left-hand side of Figure 6 to the tilted neutral line reconnection site. The density, field strength, and V_A are predicted from magnetosheath models and normalized to the values at the Cluster 3 spacecraft when it was in the magnetosheath at 0652 UT. For reconnection at the tilted neutral line ~8 R_E from the Cluster spacecraft, V_n/V_A at the reconnection site is ~0.005–0.01.

[47] The third and fourth parts of Figure 7 show the local Alfvén speed and V_n/V_A as a function of distance along the magnetic field line from the reconnection site to the Cluster 3 spacecraft. The local Alfvén speed was assumed to be constant in the derivation of equation (10). Figure 7 shows that it may decrease by as much as 50% from the spacecraft position to the reconnection site ~8–9 R_E from the spacecraft. However, equation (10) is not very sensitive to the Alfvén speed and a change of this magnitude results in a shift of only ~0.2 R_E in the distance to the reconnection site. This shift is well within the error bars in Figures 4 and 7.

[48] In section 4, it was concluded that component reconnection was occurring and the tilted neutral line could be >8 R_E from the spacecraft (Figure 6, top right-hand side). Under these conditions, the bottom part of Figure 7 shows that V_n/V_A = ~0.005–0.01.

6. Discussion

[49] In this paper, a new multispacecraft procedure for computing the inflow velocity and the distance to the reconnection site was introduced. With two spacecraft in a reconnection layer and separated by a sufficient distance, the inflow velocity normal to the magnetopause and the distance to the reconnection site are computed using the assumption that the reconnection region can be reduced to a two dimensional geometry. These two quantities are not computed independent of one another, so additional information is required to separate them. The distance between the spacecraft is critical for the application of this technique. The distance must be large enough such that the cutoff velocities V_{e1} and V_{e2} in equation (10) differ by several hundred km/s. Of all the restrictions on this technique, this requirement on the cutoff velocities probably limits the application of this technique the most. The technique requires relatively low reconnection rates that produce $V_n/V_A \sim 0.1$, which in turn produce relatively thin boundary layers. For thin boundary layers, it is difficult to find times when two spacecraft are sufficiently separated to produce relatively large differences in the cutoff velocities V_{e1} and V_{e2} in equation (10) and yet both spacecraft are still making simultaneous observations in the boundary layer.

[50] Because of the requirements on V_{e1} and V_{e2}, it is difficult to find events that can be analyzed. Further work is needed to determine if this technique can be regularly applied to the magnetopause or if it has limited applicability similar to other techniques for determining the proxies for reconnection rate at the magnetopause.

[51] By searching the early Cluster data for times when the spacecraft had sufficient separation, an event (see Figure 3) (out of 14 events surveyed) was identified to test this two-spacecraft technique. For this event, the additional information needed for a separate determination of the distance to the reconnection site comes from the flow velocities observed simultaneously in the magnetosheath and LLBL and from the ionospheric signature of the reconnection line.

[52] These observations and models for the magnetosheath and magnetospheric magnetic fields were used to conclude that component reconnection was occurring at the magnetopause and the reconnection line (the tilted neutral line) was relatively far from the spacecraft. The precise distance was not obtained; however, it could have been >8 R_E from the spacecraft (Figure 6, right-hand side). Combining magnetosheath magnetic field and plasma models with observations at one point in the magnetosheath, the Alfvén speed as a function of distance along the magnetic field from the spacecraft to the reconnection site was computed (Figure 7). From this speed and the inflow velocity determined from the multi-spacecraft procedure, it was concluded that V_n/V_A = ~0.005–0.01 if reconnection was occurring at the relatively distant tilted neutral line.

[53] Since the exact distance to the reconnection line is not known, the estimate of $V_n/V_A \sim 0.005-0.01$ obtained from Figure 7 should be considered a minimum value. If the tilted neutral line is not straight, but curves toward higher latitudes away from the subsolar region, then the distance to the reconnection line would be reduced and V_n/V_A would increase. However, the bottom panel of Figure 7 shows that even if the reconnection site was $\sim 2\ R_E$ from the spacecraft (i.e., very nearly anti-parallel reconnection), V_n/V_A would be only ~ 0.02. Thus for this component reconnection case, the reconnection rate was a factor of 5 to more than 10 times less than the rate typically quoted for magnetopause reconnection.

[54] This ratio is considerably lower than some ratios obtained previously [e.g., *Sonnerup et al.*, 1981; *Phan et al.*, 2001]. However, this ratio is not inconsistent with a statistical study of magnetopause motion that suggests $V_n/V_A < 0.1$ [*Phan and Paschmann*, 1996] and one estimate of $V_n/V_A = \sim 0.02$ very near a diffusion region encounter [*Mozer et al.*, 2002]. For this encounter with the diffusion region, it was also concluded that component reconnection was occurring. Although many more events are needed, one possibility is that low reconnection rates are associated with component reconnection at the magnetopause, while higher reconnection rates are associated with antiparallel reconnection.

[55] **Acknowledgments.** The Cluster and IMAGE missions are the result of work of many dedicated scientists and engineers. The PI for the CIS experiment is Henri Rème and the PI for the IMAGE mission is James Burch. Data from the magnetometer and solar wind experiments on the ACE spacecraft were obtained from the CDAWeb. The PIs for these instruments are Norm Ness and Dave McComas, respectively. Research at Lockheed Martin was supported by NASA contract NAS5-30302 and NASA grant NAG5-12218 and also by subcontract through the University of California, Berkeley. The authors thank the referees for important suggestions and corrections to this paper.

[56] Lou-Chuang Lee thanks Stanley Cowley and Forrest S. Mozer for their assistance in evaluating this paper.

References

Balogh, A., et al. (1997), The Cluster magnetic field investigation, *Space Sci. Rev.*, *71*, 5.

Cowley, S. W. H. (1982), The causes of convection in the Earth's magnetosphere: A review of developments during the IMS, *Rev. Geophys.*, *20*, 531.

Cowley, S. W. H., and C. J. Owen (1989), A simple illustrative model of open flux tube motion over the dayside magnetopause, *Planet. Space Sci.*, *37*, 1461.

Crooker, N. U. (1979), Dayside merging and cusp geometry, *J. Geophys. Res.*, *84*, 951.

Dunlop, M. W., et al. (2001), Cluster observes the Earth's magnetopause: Co-ordinated four-point magnetic field measurements, *Ann. Geophys.*, *19*, 1449.

Farrugia, C. J., et al. (1988), A multi-instrument study of flux transfer event structure, *J. Geophys. Res.*, *93*, 14,465.

Fuselier, S. A., D. M. Klumpar, and E. G. Shelley (1991), Ion reflection and transmission during reconnection at the Earth's subsolar magnetopause, *Geophys. Res. Lett.*, *18*, 139.

Fuselier, S. A., B. J. Anderson, and T. G. Onsager (1995), Particle signatures of magnetic topology at the magnetopause: AMPTE/CCE observations, *J. Geophys. Res.*, *100*, 11,805.

Fuselier, S. A., S. M. Petrinec, and K. J. Trattner (2000), Stability of the high-latitude reconnection site for steady northward IMF, *Geophys. Res. Lett.*, *27*, 473.

Fuselier, S. A., S. B. Mende, T. E. Moore, H. U. Frey, S. M. Petrinec, E. S. Claflin, and M. R. Collier (2003), Cusp dynamics and ionospheric outflow, *Space Sci. Rev.*, *109*, 285.

Gonzalez, W. D., and F. S. Mozer (1974), A quantitative model for the potential resulting from reconnection with an arbitrary interplanetary magnetic field, *J. Geophys. Res.*, *79*, 4186.

Gosling, J. T., M. F. Thomsen, S. J. Bame, R. C. Elphic, and C. T. Russell (1990), Plasma flow reversals at the dayside magnetopause and the origin of asymmetric polar cap convection, *J. Geophys. Res.*, *95*, 8093.

Kobel, K., and E. O. Flückiger (1994), A model of the steady state magnetic field in the magnetosheath, *J. Geophys. Res.*, *99*, 23,617.

Levy, R. H., H. E. Petschek, and G. L. Siscoe (1964), Aerodynamic aspects of the magnetospheric flow, *AIAA J.*, *2*, 2065.

Lindqvist, P.-A., and F. S. Mozer (1990), The average tangential electric field at the noon magnetopause, *J. Geophys. Res.*, *95*, 17,137.

Lockwood, M., and M. F. Smith (1996), Earth's magnetospheric cusps, *Rev. Geophys.*, *34*, 233.

Mende, S. B., et al. (2000), Far ultraviolet imaging from the IMAGE spacecraft. 2. Wideband FUV imaging, in *The IMAGE Mission*, edited by J. L. Burch, pp. 271–285, Springer, New York.

Mozer, F. S., S. D. Bale, and T. Phan (2002), Observations of ion and electron diffusion regions at a sub-solar magnetopause reconnection event, *Phys. Rev. Lett.*, *89*, 015002.

Onsager, T. G., and S. A. Fuselier (1994), The location of magnetic reconnection for northward and southward interplanetary magnetic field, in *Solar System Plasmas in Space and Time*, *Geophys. Monogr. Ser.*, vol. 84, edited by J. L. Burch and J. H. Waite Jr., p. 183, AGU, Washington, D. C.

Paschmann, G., I. Papamastorakis, W. Baumjohann, N. Sckopke, C. W. Carlson, B. U. Ö. Sonnerup, and H. Lühr (1986), The magnetopause for large magnetic shear: AMPTE/IRM observations, *J. Geophys. Res.*, *91*, 11,099.

Petrinec, S. M., and S. A. Fuselier (2003), On continuous versus discontinuous neutral lines at the dayside magnetopause for southward interplanetary magnetic field, *Geophys. Res. Lett.*, *30*(10), 1519, doi:10.1029/2002GL016565.

Petrinec, S. M., and C. T. Russell (1997), Hydrodynamic and MHD equations across the bow shock and along the surfaces of planetary obstacles, *Space Sci. Rev.*, *79*, 757.

Petrinec, S. M., T. Mukai, A. Nishida, T. Yamamoto, and T. K. Nakamura (1997), Geotail observations of magnetosheath flow near the magnetopause, using Wind as a solar wind monitor, *J. Geophys. Res.*, *102*, 26,943.

Phan, T.-D., and G. Paschmann (1996), Low-latitude dayside magnetopause and boundary layer for high magnetic shear: 1. Structure and motion, *J. Geophys. Res.*, *101*, 7801.

Phan, T. D., B. U. Ö. Sonnerup, and R. P. Lin (2001), Fluid and kinetics signatures of reconnection at the dawn tail magnetopause: Wind observations, *J. Geophys. Res.*, *106*, 25,489.

Rème, H., et al. (2001), First multispacecraft ion measurements in and near the Earth's magnetosphere with the identical cluster ion spectrometry (CIS) experiment, *Ann. Geophys.*, *19*, 1303.

Sonnerup, B. U. O. (1974), Magnetopause reconnection rate, *J. Geophys. Res.*, *79*, 1546.

Sonnerup, B. U. Ö., and B. G. Ledley (1979), Electromagnetic structure of the magnetopause and boundary layer, in *Magnetospheric Boundary Layers*, *ESA SP-148*, edited by B. Battrick, p. 401, Eur. Space Agency, Paris.

Sonnerup, B. U. Ö., G. Paschmann, I. Papamastorakis, N. Sckopke, G. Haerendel, S. J. Bame, J. R. Asbridge, J. T. Gosling, and C. T. Russell (1981), Evidence for magnetic field reconnection at the Earth's magnetopause, *J. Geophys. Res.*, *86*, 10,049.

Swisdak, M., B. N. Rogers, J. F. Drake, and M. A. Shay (2003), Diamagnetic suppression of component magnetic reconnection at the magnetopause, *J. Geophys. Res.*, *108*(A5), 1218, doi:10.1029/2002JA009726.

Trattner, K. J., S. A. Fuselier, and S. M. Petrinec (2004), Location of the reconnection line for northward interplanetary magnetic field, *J. Geophys. Res.*, *109*, A03219, doi:10.1029/2003JA009975.

Tsyganenko, N. A. (1995), Modeling the Earth's magnetospheric magnetic field confined with a realistic magnetopause, *J. Geophys. Res.*, *100*, 5599.

S. A. Fuselier, S. M. Petrinec, and K. J. Trattner, Lockheed Martin Advanced Technology Center, 3251 Hanover Street, Palo Alto, CA 94304-1191, USA. (fusilier@spasci.com)

C. J. Owen, Mullard Space Science Laboratory, University College London, Holmbury St. Mary, Dorking, Surrey, RH5 6NT, UK.

H. Rème, CESR/CNES, BP4346, F-31028 Toulouse, France.